IEEE Access
Multidisciplinary | Rapid Review | Open Access Journal

Received March 19, 2019, accepted April 2, 2019, date of current version May 6, 2019.

Digital Object Identifier 10.1109/ACCESS.2019.2911260

Predicting Damage and Life Expectancy of Subsea Power Cables in Offshore Renewable Energy Applications

FATEME DINMOHAMMADI[1], DAVID FLYNN[1], CHRIS BAILEY[2], MICHAEL PECHT[3], CHUNYAN YIN[2], PUSHPA RAJAGURU[2], AND VALENTIN ROBU[1]

[1]Smart Systems Group, School of Engineering and Physical Sciences, Heriot-Watt University, Edinburgh EH14 4AS, U.K.
[2]Department of Mathematical Sciences, University of Greenwich, London SE10 9LS, U.K.
[3]Center for Advanced Life Cycle Engineering (CALCE), University of Maryland at College Park, College Park, MD 20742, USA

Corresponding author: Fateme Dinmohammadi (f.dinmohammadi@hw.ac.uk)

This work was supported in part by the SSE plc (http://sse.com/). The work of F. Dinmohammadi, D. Flynn, and V. Robu was supported in part by the EPSRC Project on HOME-Offshore under Grant EP/P009743/1, and in part by the Engineering and Physical Sciences Research Council (EPSRC) Offshore Robotics for Certification of Assets Hub under Grant EP/R026173/1.

ABSTRACT Subsea power cables are critical assets within the distribution and transmission infrastructure of electrical networks. Over the past two decades, the size of investments in subsea power cable installation projects has been growing significantly. However, the analysis of historical failure data shows that the present state-of-the-art monitoring technologies do not detect about 70% of the failure modes in subsea power cables. This paper presents a modeling methodology for predicting damage along the length of subsea cables due to environmental conditions (e.g., seabed roughness and tidal flows) which result in the loss of the protective layers on the cable due to corrosion and abrasion (accounting for over 40% of subsea cable failures). For a defined cable layout on different seabed conditions and tidal current inputs, the model calculates the cable movement by taking into account the scouring effect and then it predicts the rate at which the material is lost due to corrosion and abrasion. Our approach integrates accelerated aging data using a Taber test which provides abrasion wear coefficients for the cable materials. The models have been embedded into a software tool that predicts the life expectancy of the cable and demonstrated for narrow conditions, where the tidal flow is unidirectional and perpendicular to the power cable. The paper also provides discussion on how the developed models can be used with other condition monitoring data sets in a prognostics framework.

INDEX TERMS Offshore renewable energy, subsea cables, degradation, prognostics, life expectancy, abrasion, wear, corrosion, scour.

I. INTRODUCTION

Society and industry are increasingly becoming more dependent on the continuity of services provided by private energy companies as well as the public infrastructure sector (including national energy research or regulatory bodies). These private and public systems together build our national energy network, in which safety aspects are of great importance.

With the development of services and systems, the interdependencies between previously isolated infrastructure such as transportation systems and energy networks are expected to further increase. This is driven by increasing electrification of domestic and commercial transportation fleets. The interdependencies between critical infrastructures may cause the occurrence of cascading, escalating and common-cause failures and thereby resulting in loss of system availability [1]. The scale of this challenge can be appreciated when considering the fact that the electrical network within the United States is anticipated to require $2 trillion in upgrades and repairs by 2030 [2]. According to a report published by the UK's Department for Business, Energy & Industrial Strategy (BEIS) – formerly known as Department of Energy and Climate Change (DECC) – the power distribution and transmission network required an investment of around £34 billion between the years 2014 and 2021 [3]. Due to the high volume of investment needed to develop and maintain the existing infrastructures, the decision-makers may be tempted to defer some of the upgrading works for

The associate editor coordinating the review of this manuscript and approving it for publication was Chong Leong Gan.

as long as possible. However, this will create a demand for the development of advanced analytics tools that are capable of monitoring the health condition as well as evaluating the expected lifetime (EL) of industrial equipment and civil infrastructures.

Along with increasing the number and size of offshore renewable energy projects in different regions of the world, the global energy supply is becoming more and more dependent on reliable integration of offshore renewable energy sources into electrical grids. For example, the UK's Crown Estate has set a target of increasing the total capacity of offshore wind to 40GW at a cost of £160 billion over the next two decades [4].

Power cables are one of the most critical assets within the offshore renewable energy projects. These cables are vital to existing power distribution and transmission networks as well as for further development of offshore renewable energy installations. They play an important role in enabling the decarburization of national and international energy systems. In recent years, huge investments have been made to deploy subsea power cables for connecting UK offshore wind farms to the national grid. The Western Isles Link Interconnector required £900M of investment for the construction and installation [5]. The NorthConnect project between the UK, Norway and Sweden required 1 billion pounds capital investment (for more see [6]). More recently, the Western HVDC Link project which links the transmission network between Scotland, England and Wales incurred an estimated cost of 1 billion pounds [7].

Increasing offshore renewable energy production results in higher demand for reliable subsea power cables. It is reported that global demand for power cables will grow to an estimated length of 24,103km by 2025 [8]. This is mainly driven by the demand for offshore wind farm cables which will grow at an annual rate of 15%, accounting for 45% of the forecasted demand. Therefore, it is expected that many of the recently deployed subsea cables will require extensive repair or complete replacement in the upcoming years. This also creates a market climate in situations where wind farm power cables are prone to premature failures and manufacturers do not adapt their products for extended life operations. According to GCube Insurance Services [9], the subsea cable failures accounted for 77% of the total financial losses in global offshore wind projects in 2015. Maintaining these cables is of critical importance to utilities that face significant penalties due to power supply interruptions, lost production, or unavailability of electricity to consumers.

Currently, the installation of subsea cables in offshore renewable energy projects is carried out according to existing codes and standards centered on pipeline stability (such as DNVGL-RP-F109 [10]). However, the accuracy of such codes have never been comprehensively tested [11]. Subsea cable failures are costly to repair, and may result in significant loss of revenue due to disruption in power supply. For example, the cost for locating and replacing a section of damaged subsea cable can vary from £0.6 million to £1.2 million [12].

TABLE 1. Root causes of subsea cable failures between the years 1991 and 2006 (source: SSE PLC).

Failure causes of subsea power cables		Number of failures	% of total
Environment	Armour Abrasion	26	21.7
	Armour corrosion	20	16.7
	Sheath failure	11	9.1
Total [Environment]		**57**	**47.5**
Third-party damage	Fishing	13	10.8
	Anchors	8	6.7
	Ship contact	11	9.1
Total [Third-party damage]		**32**	**26.7**
Manufacturing/ design defects	Factory joint	1	0.8
	Insulation	4	3.4
	Sheath	1	0.8
Total [Manufacturing/design defects]		**6**	**5.0**
Faulty installation	Cable failure	2	1.6
	Joint failure	8	6.7
Total [Faulty installation]		**10**	**8.3**
Not fault found (NFF)	Unclassified	10	8.3
	Unknown	5	4.2
Total [NFF]		**15**	**12.5**
Total		**120**	**100**

To improve the understanding of power cable failure modes and to satisfy the need for development of an intelligent prognostic and health management (PHM) system for subsea cable monitoring, it is crucial to first analyses the historical failure data. Table 1 provides a list of root causes of subsea power cable failures as reported by SSE plc (http://sse.com/)-formerly Scottish and Southern Energy plc-over a 15 years period of time, between 1991 and 2006.

As shown in Table 1, the predominant failure modes of subsea power cables are associated with external factors, namely extreme environmental conditions (47.5%) and third party damage (26.7%). Armour and sheath failures are due to wear-out mechanisms such as corrosion and abrasion, whereas third party inflicted failures occur mainly due to random events such as shipping incidents or falling objects.

Traditionally, power cable manufacturers have undertaken a number of rigorous tests to verify the mechanical reliability of the cables before supplying them to customers [13]. These tests are conducted following the recommendations of the International Council on Large Electric Systems (Cigré) in Electra No. 171 [14]. This is a very popular test standard describing the procedures for evaluating torsional and bending stresses in power cables. Cigré Electra No. 171 is extensively used by industries to assess the cable mechanical strength during laying operation on the seabed. IEC 60229 standard [15] also provides a range of tests for the measurement of cable abrasion and corrosion rate. In the abrasion wear test, a cable is subjected to a mechanical rig test in which a steel angle is dragged horizontally along the cable. This test is designed to examine whether the cable can resist the damage caused during its installation. Thus, this test does not duplicate the abrasion behavior of the cable when it slides along the seabed due to tidal current.

The current commercial state-of-the-art monitoring technologies for subsea cables predominately focus on the

internal failure modes associated with partial discharge via online partial discharge monitoring, or in more advanced cable products, distributed strain and temperature (DST) measurements via embedded fiber optics. Based on analysis of the historical data from SSE plc, the existing power cable monitoring technologies only provide insight into about 30% of failure modes. As an example, with respect to partial discharge monitoring, the current technologies can only detect a failure event. This may indicate the cable is compromised as opposed to failure, but nonetheless does not represent a precursor indicator of failure. Given the logistical and accessibility challenges associated with subsea cable inspection and repair, precursor to failure can have a great impact on the reliability as well as the operating expenditure (OPEX) of subsea cables. In addition to these in-situ methods, subsea cable inspections are limited to diver observations in shallow waters or video footages which have some limitations (such as requiring good visibility, having poor accessibility to the cable) and also challenges in locating the cable.

A review of the literature reveals that very few studies have been conducted on modeling of subsea cables' failures and their wear-out mechanisms due to corrosion and abrasion [16]. In previous research, Larsen-Basse *et al*. [17] developed a model for predicting the lifetime of a cable of length 40m suspended between rocks in a deep-water section of the Alenuihaha Channel in Hawaii. The model focused on localized abrasion wear on a section of cable route hung between rocks but their model neither took into account the full length of a cable nor included the effects of corrosion and scouring. In another study, Wu [18] developed a model to predict lifetime of subsea cables by taking into account both the effects of abrasion and corrosion. However, the model required cable movement to be measured and provided as an input into the model. Booth [19] provided details on how to obtain the abrasion wear coefficient for polyethylene outer-serving by means of the Taber abrasive test. This study considered several factors affecting abrasion wear rate, such as effective coefficient of friction between the abrasive wheel and test specimen. The Taber test can be used to obtain wear rate coefficients for different seabed conditions (sand, rocks, etc.). However, data from such a test has never been used up to now in a modeling analysis.

As the above review shows, the literature on predicting the degradation of subsea cables is scarce. Given the fact that the development of offshore renewable energy projects is dependent on efficient management and integrity of subsea cable assets, there will be an urgent need for industry to provide a predictive modeling tool that is capable of calculating subsea cable movement, scouring, abrasion and corrosion in a unified manner. There are many fault diagnosis systems for subsea cables which are focused on internal failure modes due to partial discharge and localized heating from electrical overloading and/or degradation of internal insulation materials. However, these systems are not able to predict the expected lifetime (EL), of a cable section subjected to various wear-out mechanisms. To the best of the authors' knowledge, this is the first study that integrates offline experimental data from a Taber test to account for abrasion, along with an analytical model that integrates corrosion and abrasion degradation and cable displacement for in-situ conditions. The outcomes of our analysis can support cable manufacturers, offshore operators and utility companies to accurately assess the life expectancy of their cabling systems from design, to deployment and lifecycle management. Hence, in terms of maintaining such assets and assuring the continuity of energy export from offshore generation, our model can enable industry to predict the time and location of failure within a cable section (based on local seabed conditions and tidal current parameters) thereby, reducing operation and maintenance costs and minimizing the risks to this critical infrastructure.

The organization of this paper is as follows. Section II provides an overview of the structure of a subsea power cable and its key design parameters in life assessment. Section III discusses the details of sliding distance, scour, wear and lifetime models. Due to the fact there is no data available relating to varying seabed topography and friction forces on subsea cables, details on how the data from Taber tests can be sourced are described in Section IV. Section V presents the software tool 'CableLife' designed for predicting the expected life of subsea cables. Section VI presents the uncertainty associated with expected life for random input parameter such as tidal flow. Section VII concludes with a summary of the key outputs and observations within this research.

II. SUBSEA POWER CABLES

Subsea power cables are required to conduct their specific electrical loads up to a rated value and this must maintain continuously working voltage, and the cable must sustain its integrity when exposed to switching surges. There are a variety types of subsea power cables, however, the functional requirements of the dielectric materials remain consistent in terms of primary functions. These include the ability of the dielectric materials to maintain high AC and impulse electric strength, low permittivity and power factor. This will ensure lowest possible dielectric losses, physical and chemical stability over a wide range of operating temperatures. A reliable cable will have good thermal conductivity to facilitate heat transfer from the conductor and flexibility to permit bending, which is particularly important for transport and cable laying [13]. The general design requirements when procuring a power cable are related to:

(i) Single or double wire armour: taking into consideration different environmental parameters (sand, rock, strong current, etc.), shipping activities (fishing, ferries, anchorages, etc.) and installation method (direct lay, burial, rock dump, etc.);
(ii) Insulation type: Ethylene Propylene Rubber (EPR), Cross Linked Polyethylene (XLPE); etc.; and
(iii) Cable's specifications: minimum bending radius (storage and installation), maximum depth of installation, drop height and jointing (shore end and subsea).

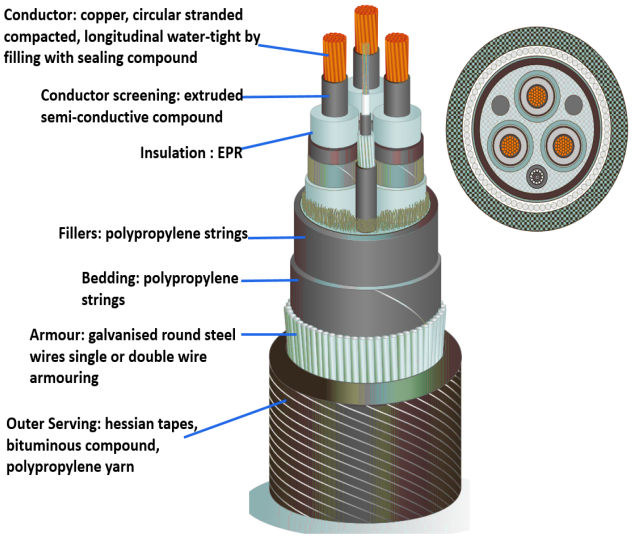

FIGURE 1. Subsea power cable construction layers [20].

Figure 1 shows the geometry and materials for a typical subsea power cable. The core copper conductors at the center of the cable are surrounded by a number of insulating layers. These insulation layers may degrade over time due to a combination of temperature, electric, chemical, and mechanical stresses. Protecting these insulation layers is accomplished using water blocking sheaths made of polymeric or metal materials. These protection layers consist of the armour (usually made of galvanized/stainless steel wires) which provides tension and compression stability, mechanical protection particularly during laying operation (installation), and from external aggression.

External aggression or third party damages are caused by cable movement on the seabed, and fishing gear and ship anchors entangling and damaging the cable. Double layer armour cable is used to provide an additional layer of protection. To protect the armour from corrosion, the final outer layer (outer serving) of the cable consists of hessian tapes, bitumen and yarn or polypropylene strings. The armour is made of galvanized steel/stainless steel, which is widely used for corrosion resistance.

The whole cable on the seabed is often subjected to different localized tidal flows and abrasion due to different seabed conditions. This will affect the local movement of the cable as well as damage due to wear in the protective layers. Hence, a mathematical model must be developed to capture these localized effects in order to accurately assess the damage to subsea cables and predict their expected life. An assessment of averaged 'global' values (e.g. not taking into account changing seabed and tidal flow conditions along the length of the cable) will result in poor (generally optimistic) predictions.

III. COMPONENTS OF THE LIFETIME PREDICTION MODEL FOR SUBSEA CABLES

This section describes the components of the developed life assessment model for subsea cables, including its capability to predict local sliding distance, scouring, and wear due to abrasion and corrosion.

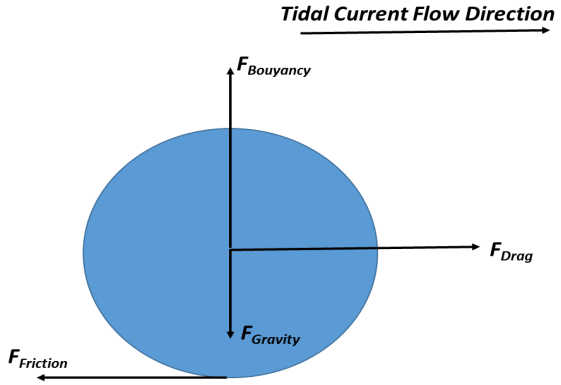

FIGURE 2. Forces acting on cable.

A. PREDICTING CABLE SLIDING DISTANCE

The mechanical forces that subsea cables experience under a tidal current are shown in Figure 2. The cables are subject to two primary dominant forces along the tidal current axis. These forces include the drag force (F_{Drag}) due to tidal flow and the frictional force (F_{Friction}) due to the seabed in the opposite direction.

In our developed model it is assumed that other forces acting on the cable such as lift force and skin friction force are negligible [21]. However, these forces will be measured and considered in a future study. Introducing lift force will reduce the abrasion wear, hence results in an increase in EL prediction. The drag force can be calculated using a widely cited equation as given in Eq. (1). Another form of this equation for cable being towed underwater was discussed by Friswell [22].

$$F_{\text{Drag}} = 0.5\rho v^2 AC, \tag{1}$$

where F_{Drag} is drag force, ρ is density of the seawater, v is velocity of the cable relative to the seawater, A is reference area, and C is drag coefficient which is dependent on Reynold's number of the fluid. In this study, the drag coefficient C is conservatively adopted as 1.2, which is a widely cited value for drag coefficient of a cylindrical immersed object [23]. The frictional force can be calculated by:

$$F_{\text{Friction}} = \left(F_{\text{Gravity}} - F_{\text{Buoyancy}}\right)\mu, \tag{2}$$

where F_{Buoyancy} is buoyancy force, F_{Gravity} is gravitational force, and μ is friction coefficient. The friction coefficient μ for subsea cables is typically between 0.2 and 0.4 [24]. If the drag force is higher than the frictional force, the cable will start moving until it reaches an equilibrium position. If the drag force F_{Drag} is lower than or equal to the frictional force F_{Friction}, the cable will not slide.

Given a tidal flow profile along the length of the cable, we have used a catenary model to predict sliding distance (d) along the cable route. The cable route is divided into a number

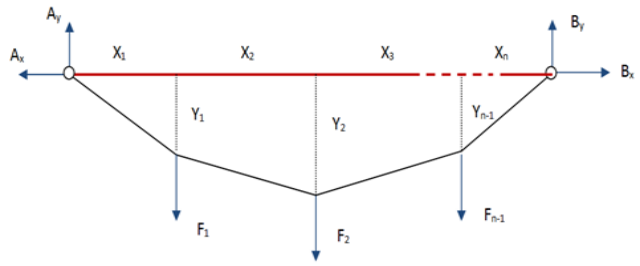

FIGURE 3. A catenary model with concentrated loadings.

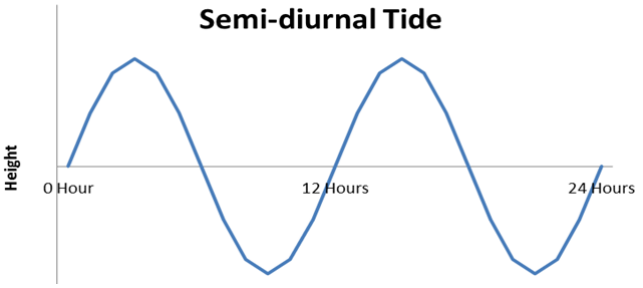

FIGURE 4. The most common tidal pattern.

of segments or zones with defined environmental (tidal flow profile) or seabed conditions at each cable zone (as illustrated in Figure 3). Hence the forces $\{F_i\}_{i=1\ldots n-1}$ depend on the tidal flow patterns and environmental factors.

The cable is fixed at both ends (A, B) and the forces experienced at longitudinal and transverse directions at these locations are A_x, A_y, B_x and B_y respectively. The length of the cable $\{\mathrm{X}_i\}_{i=1,2,\ldots n}$ in each cable zone is defined by the cable designer/installer and these zones will be governed by tidal flow and seabed conditions along the cable. Using the equation of moment equilibrium [25], the sliding distance Y_{n-1} in each cable zone can be predicted based on the following assumptions.

(i) The deformation of the cable under a tidal current is minor and can be ignored.

(ii) The displacement of the cable under a tidal current is mainly caused by the fact that the cable is slack (not tense). In this paper, we assume that the cable is 1% longer than the straight line distance between ends (A, B). The developed software allows the cable designer to input this value for each cable route.

Using the equations of moment equilibrium, we can obtain A_y and B_y as the function of forces on each cable segment and cable zone lengths by the following equations:

$$A_y = \frac{\sum_{i=1}^{n-1} F_i \sum_{j=i+1}^{n} X_j}{\sum_{k=1}^{n} X_k}, \tag{3}$$

$$B_y = \frac{\sum_{i=1}^{n-1} F_i \sum_{j=1}^{i} X_j}{\sum_{k=1}^{n} X_k}. \tag{4}$$

In addition, we have the equilibrium relationship for horizontal forces, that is, $A_x = B_x$. At each loading point, using the moment of equilibrium, we can obtain a common derivation for sliding distance by Equation (5):

$$Y_i = \frac{A_{\mathrm{y}} \sum_{j=1}^{i} X_{\mathrm{j}} - \sum_{k=1}^{i-1} F_{\mathrm{k}} \sum_{l=k+1}^{i} X_{\mathrm{l}}}{A_{\mathrm{x}}} \tag{5}$$

Due to 1% slacking ratio, the length of the equilibrium cable is equal to 1.01 times the direct distance between point A and point B. Therefore,

$$\sqrt{X_1^2 + Y_1^2} + \sum_{i=2}^{n-1} \sqrt{X_i^2 + \left(Y_i^2 - Y_{i-1}^2\right)} + \sqrt{X_n^2 + Y_{n-1}^2} = 1.01 \times \sum_{j=1}^{n} X_j. \tag{6}$$

By substituting the Y_i value (given by Equation (5)) into Equation (6), we can derive an equation for one variable of A_x. The resulting nonlinear equation can be solved by numerical root finding methods such as Ridders' algorithm or Newton-Raphson method [26] for A_x and then, the approximate sliding distances ($\{Y_i\}_{i=1\ldots n-1}$) of each cable segment can be extracted.

Figure 4 illustrates a typical 24-hour tidal flow pattern of current, which follows a semi-diurnal shape. Based on this daily tidal flow pattern, the predicted sliding distance over a 24-hour period is given by:

$$d_{Sliding} = 8 * Y_i \tag{7}$$

B. PREDICTING CABLE SCOURING DEPTH

Subsea cables are usually laid on the seabed or buried. When the cables are laid on the seabed, tidal current can cause cable scouring. This occurs when tidal current causes the sediments and sands under the cable to erode, which results in the cable to become suspended over the scour hole. Then, the cable sags into the scour hole due to its own weight and backfilling of sand follows, which eventually leads to self-burial of the cable. This phenomenon is important to be taken into account while modeling the lifetime of subsea cables, as localized regions of scouring will show very different wear behavior compared to those that are not influenced by scouring.

If the cable is self-buried due to scouring, then it cannot slide. In a steady current, the critical scouring velocity (V_{Critical}) for onset of scour can be predicted using Equation (8)(for more see Sumer and Fredsøe [27] and Arya and Shingan [28]):

$$V_{\mathrm{Critical}} = \sqrt{0.025 g d_{\mathrm{Cable}} (1-\phi)(SG-1)\, e^{\left(9\sqrt{\frac{h_{\mathrm{Initial}}}{d_{\mathrm{Cable}}}}\right)}} \tag{8}$$

where d_{Cable} is cable diameter, h_{Initial} is initial burial depth of the cable, g is acceleration due to gravity, ϕ is porosity of seabed, and SG is specific gravity of sediment grains. If the critical scoring velocity (V_{Critical}) is larger than the tidal current velocity (V_{Tidal}), then onset of cable scouring will initiate in a particular cable section.

The scour depth will increase and gradually becomes stable at its largest depth. The maximum scour depth at the equilibrium state is called equilibrium scour depth (h_{Scour}), and is

given by the following equation:

$$h_{\text{Scour}} = 0.972 d_{\text{Cable}}^2 \left(\frac{V_{\text{Tidal}}^2}{2g} \right)^2. \quad (9)$$

To calculate the time scale of the scouring process, first, undisturbed bed friction velocity ($V_{BedFriction}$) needs to be calculated. This is given by Equation (10) [29], [30]:

$$V_{BedFriction} = \frac{V_{Tidal}}{2.5 \left[ln \left(\frac{30 d_{water}}{r_{bed}} \right) - 1 \right]}, \quad (10)$$

where d_{water} is water depth, r_{bed} is seabed roughness (normally taken as 2.5 × d_{50}), and d_{50} is the representative diameter of the seabed sand/sediment grain. With known bed friction velocity ($V_{BedFriction}$), time scale for scouring (t_{scour}) is evaluated by Equation (11) (see [29], [30]):

$$t_{scour} = \frac{d_{Cable}^2}{\left(g \left(SG - 1 \right) d_{50}^3 \right)} \left(\frac{1}{50} \right) \left(\frac{V_{BedFriction}^2}{g \left(SG - 1 \right) d_{50}} \right)^{-\frac{5}{3}}. \quad (11)$$

C. CABLE WEAR MECHANISMS

Predicting wear related damage for a subsea cable requires a mathematical representation of the wear process due to both abrasion and corrosion. We assume abrasion and corrosion are independent to each other. These models are discussed below:

Abrasion Wear Rate: Abrasion is a wear mechanism of the cable outer layer due to cable sliding along the rough seabed. A detailed list of different abrasive wear models for plastic materials can be found in Budinski [31]. In this study, the widely used Archard abrasion wear model has been adopted [32]. In this model, the wear volume is proportional to the sliding distance, as given in the Equation (12):

$$V_A = k \frac{F_{Cable} d_{Sliding}}{H}, \quad (12)$$

where V_A is wear volume per day (m^3/day) due to abrasion, F_{Cable} is cable weight in water (N), $d_{Sliding}$ is sliding distance per day(m/day) which is calculated using Eq. (7), H is hardness (N/m^2), and k is wear coefficient for each layer in the cable which is obtained experimentally from Taber test

Corrosion Wear Rate: To calculate the corrosion wear, the following equation is used [33]:

$$V_{\text{C}} = c_1 A_{\text{Exposed}} \left(t - T_{\text{Coating}} \right)^{c_2}, \quad (13)$$

where V_{C} is wear volume per day due to corrosion (m^3/day), A_{Exposed} is exposed area of the material to seawater, t is elapsed time (day) after the cable is laid, T_{Coating} is life of the coating (time scale of coating to disintegrate, since the coating acts as a barrier to oxygen and water reaching the surface of the material), c_1 is corrosion penetration rate per day (m/day), and c_2 is usually assumed as 1/3 or pessimistically assumed to be one. The corrosion rate c_1 is the corroded/pitted depth per day which is assumed for carbon steels in seawater to be 4 mm/year (see API RP-2SK [34] and [35], [36]). For stainless steel, average corrosion penetration rate is adopted as 0.07 mm/year [37].

If the equilibrium scour depth in a zone h_{Scour}, given in Equation (9), is greater than cable radius, then we assume that the cable will become buried and will not experience sliding and abrasion at that zone. Hence, wear-out damage of the cable in that section will be due to corrosion on the armour layer only.

D. PREDICTING CABLE LIFETIME

Based on a pre-defined tidal flow, we use the catenary approach and scouring model to calculate cable sliding distance ($d_{Sliding}$) at different sections of the cable, given by Eq.(7). Using this value of sliding distance at each section, together with a measured abrasion wear coefficient (k) (e.g. from Taber test),we can calculate volume of material lost due to abrasion over time ($V_{Abrasion}$) by Equation (12).

Given the corrosion rate for different cable materials, we can calculate the material loss due to corrosion ($V_{\text{Corrosion}}$) by Equation (13). By combining these predictions for material loss due to abrasion and corrosion, we develop a model to predict the life expectancy of the subsea cable.

In this paper, the threshold for cable failure is when the protective layers on the cable (polypropylene yarn and armour) have been lost due to corrosion and abrasion. Hence the Expected life (EL) of the cable is the length of time the cable will operate before the insulation layer become exposed due to removal of the external protective layers.

Based on tidal flow data, the above models can predict the rate at which protective layers ($j = 1{:}N$) are lost due to abrasion (e.g V_A^j) and corrosion (V_C^j). The total wear rate for each of the protective layers (polypropolyne yarn and armour) equals to $V_A^j + V_C^j$. These are calculated based on the exposed areas of the cable to the failure mechanisms as shown in Figure 5. The total volume that can be lost due to corrosion and abrasion for each layer (j) (as illustrated in Figure 5) is given by V_T^j. Hence, expected life for each protective layer i (EL_i) is given by:

$$EL_i = \sum_{j=1}^{i} \frac{V_T^j}{\left(V_A^j + V_C^j \right)}, \quad (14)$$

where the rate of volume loss due to abrasion is considered as function of seabed roughness, tidal flow, etc. Figure 5 depicts three protective layers (*Bitumen, $j = 1$; Polypropylene, $j = 2$; Steel Armour, $j = 3$)* that needs to be considered in predicting material loss due to interaction with the seabed. For bitumen type of material, the corrosion wear can be neglected. Hence, the wear will be dominated by abrasion. In order to predict the lifetime of the cable, we need to calculate the maximum volume that can be lost for each layer. This is the threshold value used to indicate cable failure. Given the rotation impacts are negligible, the lost volume from the layer is calculated using the following equations:

$$V_{33} = (r - h_1 - h_2)^2 \frac{(\theta_3 - Sin(\theta_3))}{2}, \quad (15)$$

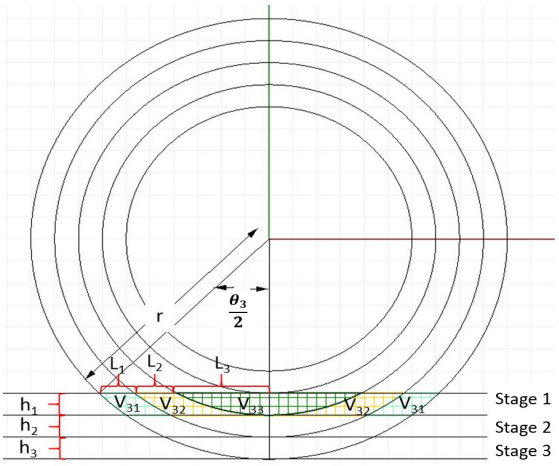

FIGURE 5. Schematic view of layer volumes in three stages.

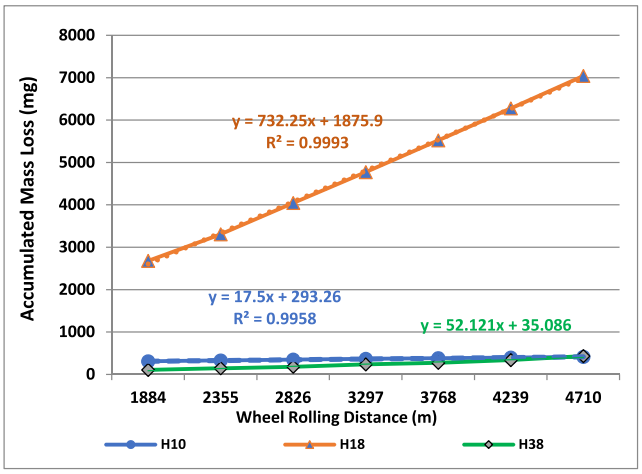

FIGURE 6. Stainless steel accumulated volume loss plot versus Taber abrasive wheel rolling distance.

where,

$$\theta_3 = 2Cos^{-1}\left(\frac{r - h_1 - h_2 - h_3}{r - h_1 - h_2}\right). \tag{16}$$

The time to failure of the third layer is defined as the ratio between total volume of the third layer and the sum of corrosion and abrasion wear rates per day, that is,

$$\frac{V_{33}}{\frac{k_3 C F_{Cable} d_{Sliding}}{H_3} + c_{31} L_3 \left(t - T_3^{Coating}\right)^{c_{32}}}, \tag{17}$$

where $C = \frac{L_3}{L_1+L_2+L_3}$, H_3 is hardness of the third layer material, k_3 is abrasion coefficient of the third layer material, $d_{Sliding}$ cable sliding distance in one day, $T_3^{Coating}$ is corrosion resistance coating time of the third layer material, t is the elapsed time (days) after laid, c_{31} is corroded/pitted depth of third layer material per day, c_{32} is constant for third layer material of the corrosion wear model in Equation (12), V_{33} is volume of the third layer, θ_3 is an angle shown in Figure 5, F_{Cable} is the cable weight in water, and L_1, L_2, L_3 are the cross sectional lengths of three stages shown in Figure 5.

In Figure 5, h_1, h_2, and h_3 represent thicknesses of the first, second and third outer layers of the cable. In a similar way, the failure time can be derived for each layer volume (V_{32} and V_{31}) on each stages. Complete failure is assumed to occur once the armour layer of the cable is worn out.

IV. TABER ABRASIVE EXPERIMENT

In order to predict the wear volume of the cable layer due to abrasive wear in Equation (12), wear coefficient k needs to be identified for each layer of materials in the cable when subjected to varying seabed material interfaces. At the time of investigation, there was no data available within industry or academia relating to these wear coefficients. In consultation with the British Approvals Service for Cables (BASEC) (https://www.basec.org.uk/), a material test was designed and undertaken to measure these wear coefficients. It should be noted that subsea cable testing standards for abrasion are defined for the cable laying process, and these standards do not consist of the specifications for long-term reliability assessment of cables. Hence, in this study, we adopted the current Taber test technique to extract abrasion wear coefficients for a cable with different seabed conditions.

The outer layer of the subsea cable consists of an outer serving and armour wire. The outer serving is made of polypropylene and bitumen and will wear much more quickly than the armour due to abrasion wear. The outer serving consists of two layers, namely the polypropylene and bitumen impregnated polypropylene. The polypropylene, bitumen and steel armour test samples in flat sheet form were sourced from the cable manufacture. These samples were utilized in the Taber abrasive experiment. The Taber 5130 abrader machine was used and the experiments were undertaken according to the ASTM D4060-10 standard [38]. Three abrasive wheel types such as H10 (designed to provide coarse particle abrasion), H18 (designed to provide medium coarse particle abrasion) and H38 (designed to provide very fine particle abrasion) were used in the experiment. Figure 6 shows the accumulated volume losses of the stainless steel test sample (mg) versus the wheel sliding distance (m) for each of these wheel types. Hardness of stainless steel is 1372 Nmm^{-2}. Density of the stainless steel is 7850 kgm^{-3}. The wheel travel distance in a cycle is the circumference distance in center of the abrasive wear path (see Booth [39]). The test results were used to identify the wear coefficient k_s for the stainless steel. The Equation (12) is utilized to extract the steel wear coefficient k_s.

The Taber abrasive tests were also undertaken for bitumen and polypropylene samples. Hardness of polypropylene varies in the range of 36 to 70 Nmm^{-2} [40]. Density of the polypropylene is 946 kgm^{-3}. Hardness and density of bitumen were taken as 0.47 Nmm^{-2} [41] and 1050 kgm^{-3} respectively. The wear coefficient k of all three layer materials for three abrasive wheel types H10, H18 and H38 are given in Table 2. One of the outer layers consists of

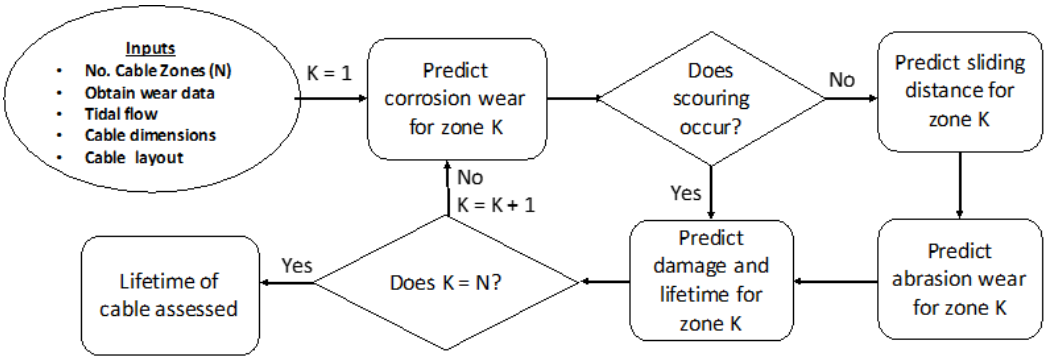

FIGURE 7. High-level illustration of CableLife modeling tool for EL prediction of subsea cables.

TABLE 2. Wear coefficients of layer materials from taber experiments.

Wheel Type	*Wear Coefficient of Polypropylene*	*Wear Coefficient of Bitumen*	*Wear Coefficient of Stainless steel*
H10	6.548×10^{-4}	4.21×10^{-5}	6.628×10^{-4}
H18	8.8308×10^{-4}	1.703×10^{-5}	2.773×10^{-2}
H38	8.35×10^{-5}	1.078×10^{-5}	1.974×10^{-3}

bitumen-impregnated polypropylene, hence it is possible to treat this layer as composite material layer.

The wear coefficient of the composite material (k_c) is derived from the inverse rule (see [42]) given in Equation (18):

$$k_c = \frac{1}{\left(\frac{V_b}{k_b} + \frac{V_p}{k_p}\right)}, \tag{18}$$

where V_b is volume fraction of bitumen, V_p is volume fraction of polypropylene, k_b is wear coefficient of bitumen, and k_p is wear coefficient of polypropylene. The experiments were undertaken once for each sample materials, hence statistical variations on the obtained coefficients values are unknown. Primary difficulties of extracting the actual wear coefficients between the subsea cable and the seabed from the wear coefficients obtained from Taber abrasive experiment are illustrated below:

- Water molecules can act like a lubricant between cable and seabed in comparison with severe dry test in Taber abrasive machine.
- In the Taber abrasive experiment, the wear is dominated by rolling friction. In contrast, the cable/seabed wear is dominated by sliding friction.

Ideally, a factor should be multiplied to the wear coefficient from Taber test to represent the true wear coefficient between the cable and seabed, but there is negligible literature on this topic. Inclination and declination of seabed landscape can also affect the abrasive wear on cable since the force of drag and friction will change. If the seabed is sandy, then when the cable slides on the seabed, the sandy seabed will deform and cause the friction coefficient μ used in the Equation (2) to change as well. A further study needs to be conducted in order to convert the Taber results and include such factors.

V. DESKTOP TOOL: CABLELIFE

Our modeling methodology for development of a software tool to predict the expected life (EL) of subsea power cables is illustrated in Figure 7. The modeling methodology has been coded into a software tool, called "CableLife". The software's Graphical User Interface (GUI) is depicted in Figure 8. The software code was written in Visual Basic for Applications (VBA) and was linked to a database containing different cable designs, layouts and cable properties. The tool can be used by designers to assess the impact of different cable layouts and tidal flow patterns on cable wear by both corrosion and abrasion at the early stages of design and deployment. As shown in Figure 8, the cable length was split into 13 zones. Based on a specific tidal flow profile, the above models report the expected life (EL) for each zone in years on the Y axis.

A. CASE STUDY

Cable sections are divided into many subsections (zones) according to the environmental factors. Initially for each zone, the critical velocity for scour is evaluated and compared with tidal flow velocity and if the tidal flow velocity is greater than critical scour velocity, then equilibrium scour depth (h_{Scour}) is evaluated using the Equation (9). If the equilibrium scour depth is greater than the radius of the cable then the cable will be self-buried. Separate catenary models on both sides of the buried cable sections are formed. This process is repeated close to zones where the cable is self-buried. Then based on catenary model as detailed in Section III, the sliding distances are predicted for each zone. Abrasion wear of cable zones are predicted using the sliding distance data. Cable lifetime is predicted for each zone due to abrasion on all protective layers and additionally corrosion wear for armour protective layer. In this case study we have two layers or protection: Polypropylene Yarn and steel armour. Hence, expected lifetime of the cable is defined as

$$EL_{Cable} = EL_{Polypropylene} + EL_{Armour}$$

To illustrate the modeling approach, an application of the CableLife software tool to a cable route is provided. The data used for this case study is based on offline experimental

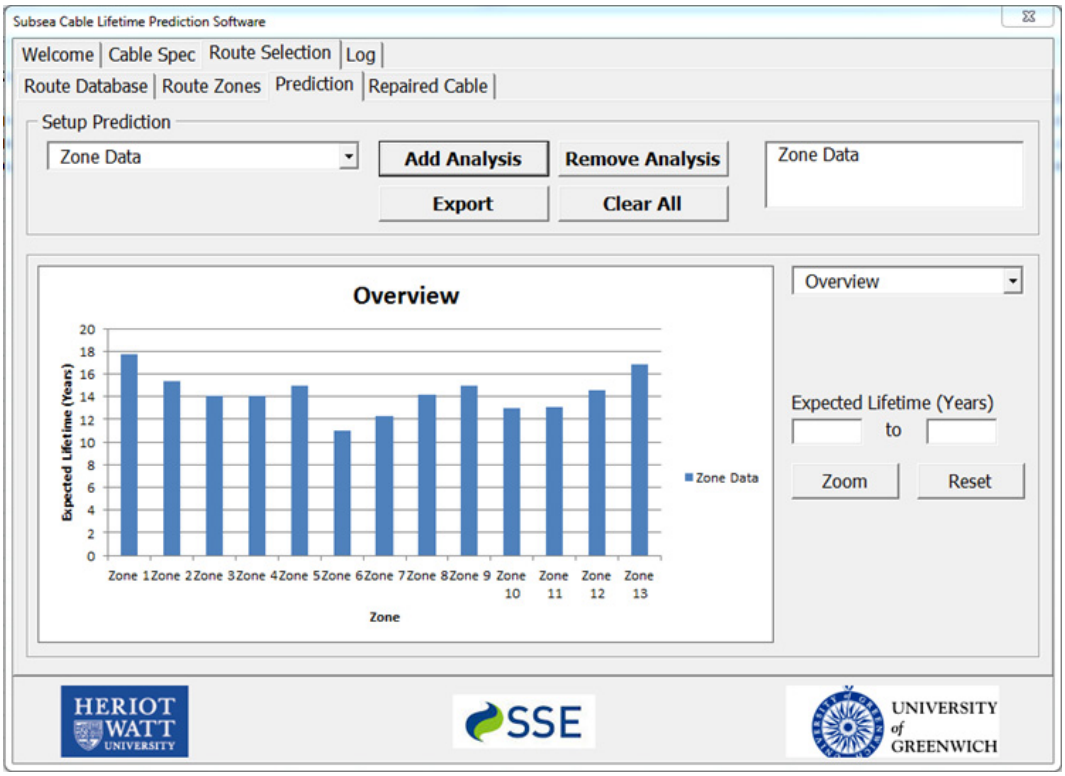

FIGURE 8. CableLife software's graphical user interface (GUI) for EL prediction of subsea power cables.

TABLE 3. Cable specifications of a single armour cable.

Physical properties	Value
Overall diameter of the cable	119 mm
Unit cable weight	21.6 kg
Thickness of first outer layer (Polypropylene)	4 mm
Thickness of second outer layer (Armour)	4 mm

lifecycle data as outlined in section IV. The length of the route between two islands was assumed as 2.1km. The length of the cable is 1% higher than the length of the route. The abrasion wear data for the cable was obtained from the Taber experiment, as presented in Table 2. The route was divided into 13 zones with varying fictional tidal flow currents ranging from 1 to 2 m/s. The cable specification used in this study is obtained from the Nexans high voltage (30kV) subsea cables brochure [43], which is given in Table 3.

Cable failure occurs when the protective armour layer of the cable is worn out. Assume that the section of the cable at zone 7 was self-buried due to scouring effect on that zone. Hence the segment in zone 7 would not slide. From the sliding distance derivation, the maximum sliding distance of the cable was identified as 60.5m at zone four. The schematic plot of the sliding distances and the tidal current flow rate of each zone are shown in Figure 9. The EL prediction plots of single armour layer cable under same environmental conditions for zone four (worst zone) are illustrated in Figure 10. The EL plots were extracted by varying the wear coefficient values of cable layer materials derived from the Taber experiments represent different seabed conditions. Doubling the armour layer increases the weight of the cable and also diameter of the cable. Hence, the sliding distance will be lower for double layer armour cable and higher expected lifetime.

VI. INCLUDING UNCERTAINTY

The above modeling methodology provides subsea cable installers with the capability to estimate to expected life (EL) of a cable based on knowledge of tidal flows and seabed conditions for a planned cable route. The methodology follows the following steps:

1) ***Route Planning:*** *Select a particular cable type (e.g. construction) and identify options for subsea cable routes.*

2) ***Data Gathering:*** *For each route obtain data of historical tidal flows,and data for corrosion and abrasion (e.g. Taber test) for each protective layer in the cable.*

3) ***Simulation:*** *Predict sliding distance and rates of corrosion and abrasion along the length of the cable. Predict the expected life of the cable based on time it takes for the insulation layers of the cable to be exposed.*

4) ***Customer Requirements:*** *Does choice of cable construction and cable route meet requirements. If not, then repeat steps (1)-(3) with new cable construction and/or route.*

The above case study made a number of assumptions with regard input values for the models. For example, the model

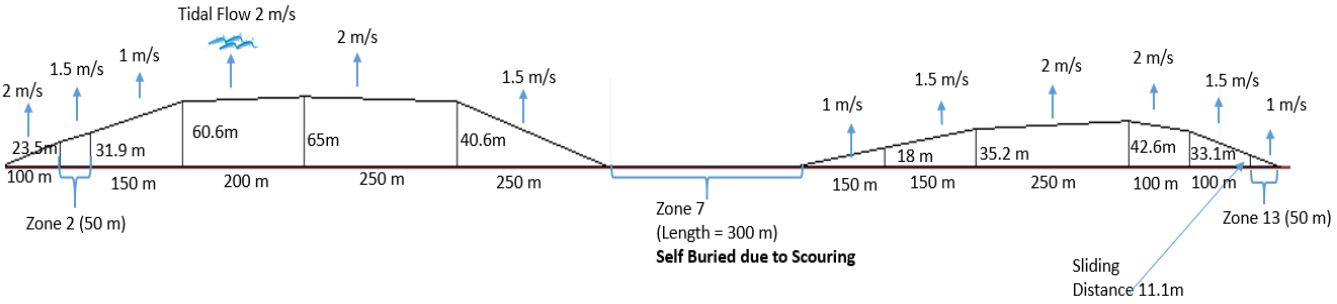

FIGURE 9. The schematic plot of the sliding distances, lengths, and the tidal current flow rate of the each zones.

used mean tidal current magnitude. However, this together with several other input parameters will be stochastic in nature. For example variability in tidal flow over time will impact sliding distance and hence abrasion of the cable. Thus, the effect of uncertainty can be incorporated into the methodology. With the availability of historical data (for example, on tidal flow), it is possible to capture this variability and evaluate its impact on life expectancy of the cable. For example, if we assume a standard deviation of sliding distance is 10% of the mean value (mean value is the evaluated value at zone 4, 60.5m) and its uncertainty follows a Gaussian distribution, then the prediction of remaining life will have stochastic distribution.

Generally sampling based approximation technique such as Monte Carlo sampling (MCS) are utilized to evaluate the uncertainty of a response dependent on random input variables. For simplicity, we employed First Order Second Moment method (FOSM) [44]. FOSM is based on first order Taylor expansion of the response at the mean values of the input random variables. By taking the first and second terms of the Taylor expansion, response is approximated as linear function. The modified response along with the two moments of input random variables, the first two moments (mean and variance) of the response is approximated.

Mean and standard deviation of the expected lifetime of the cable, EL_{Cable} is approximated by FOSM as

$$\mu_{EL_{Cable}} = EL_{Cable}\left(\mu_D\right)$$
$$\sigma^2_{EL_{Cable}} = \left(\frac{\partial EL_{Polypropylene}\left(\mu_d\right)}{\partial d}\sigma_d\right)^2 + \left(\frac{\partial EL_{Armour}\left(\mu_d\right)}{\partial d}\sigma_d\right)^2$$

where μ_d, is the mean value of the sliding distance and σ_d is the standard deviation of the sliding distance d. The first two moments of the input random variable sliding distance and EL_{Cable} are given in the Table 4. Assuming the distribution of EL_{Cable} follows a Gaussian distribution, then 95% confidence interval for EL_{Cable} distribution is obtained as $\{\mu_{EL_{Cable}} - 1.96\sigma_{EL_{Cable}}, \mu_{EL_{Cable}} + 1.96\sigma_{EL_{Cable}}\}$, Hence, the upper and lower bounds of 95 % confidence interval for

TABLE 4. Mean and standard deviation of the input variable (sliding distance) and the cable EL.

	d	EL_{Cable} (Years)
Mean	60.5	6.57
Standard Deviation	6.05	0.475

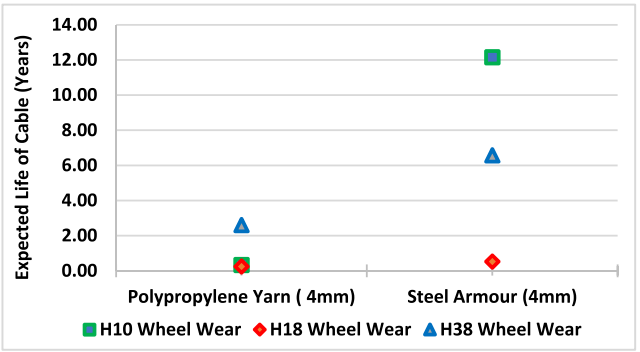

FIGURE 10. Expected life prediction of single armour layer cable at zone 4 using wear coefficient extracted from H10, H18, and H38 Taber abrasive wheels.

the cable's lifetime for H38 wheel abrasive coefficient are shown in Fig 11.

At present, the information on uncertainty distribution of these parameters or variables are unavailable. In future, the developed methods will be extended for taking into account different "uncertainties" (both aleatory and epistemic) in the prediction of EL of subsea power cables.

In the context of prognostics, the above models address a significant gap in remaining useful life (RUL) predictions of installed and planned subsea power cables. The model predictions can be integrated with other condition monitoring data sets, which focus on other failures modes such as dielectric insulation breakdown, in order to provide a more holistic RUL estimate. The summation of the estimate life based on individual failure modes would involve the following steps;

1) Input power cable manufacturer information and cable length into the offline cable model.
2) Enter environmental data relating to seabed topography and materials, as well as tidal information.

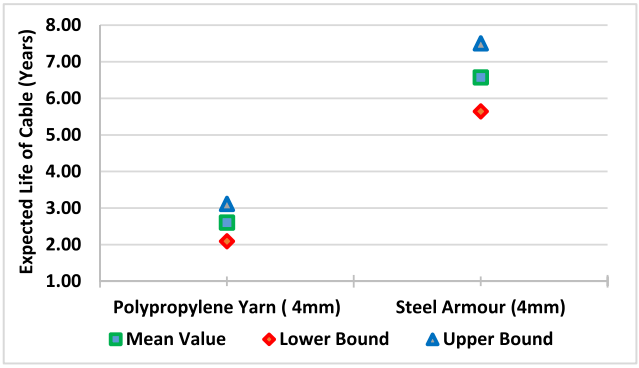

FIGURE 11. Upper and lower bound of the expected life prediction of cable at zone 4 using wear coefficient extracted from H38 Taber abrasive wheel.

3) Electrical Condition Monitoring: Data from DTS or Partial Discharge Monitoring can be used to infer the integrity of the dielectric material and precursors to failure.
4) Environmental Condition Monitoring – Abrasion and Corrosion offline predictions based on current time installed,
5) Third party (random) events; If this occurs cable displacement associated with anchor or seabed debris impact can inform a material loss estimate. Submitted into step (4)
6) Summation of Estimate Life (1-4) into an integrated remaining useful life prediction.

In addition, the current model can also utilize in-situ monitoring, either from displacement sensors which can be included into calculations for predicting the remaining useful life of a cable where the sensors placed along the cable can provide data (e.g. magnitude of local tidal currents) which the models can use to predict sliding distance and wear rates at that point time. Alternatively, direct integrity data of the subsea power cable can be obtained for low frequency sonar detection [45] With regards Equation 14, the values of abrasion rate, V_A^j, corrosion rate, V_C^j, and total volume, V_T^j, that can be lost due to corrosion and abrasion for each layer (j) will change over time and take into account material loss at previous readings and predictions.

VII. CONCLUSIONS AND FUTURE WORK

This study discussed historical failure data for subsea-power cables over a 15 years period of time, and the associated technologies used for their health monitoring. According to the analysis of historical data, it was found that about 70% of failure modes were not detected by state-of-the-art monitoring systems.

This paper details a mathematical model which can predict key physical phenomena that affects subsea power cable life (e.g. corrosion and abrasion). The model has been incorporated into a software tool – CableLife – and demonstrated for a particular cable design. The significance of this work is:

- First mathematical model to combine the effects of scour, corrosion, abrasion in a single cable life prediction model.
- Expected life prediction of subsea cables based on real physical phenomena as addressed by the above models.
- Ability of model to address significant number of cable failures due to environmental conditions (abrasion, corrosion, etc.).
- First time Taber test has been used to characterize seabed conditions and obtain wear rates for different cable materials.
- First digital predictive tool for predicting degradation and wear in subsea power cables.
- Ability of model to be embedded into prognostics environment for holistic management of subsea cables, and optimization of their installation planning.

The developed cable life assessment tool can provide a valuable capability in prognostics and health management (PHM) of existing installations as well as permitting verification of varying cable products and installation routes. The model was able to predict underwater cable movement which included the effects of scouring based on tidal flow profiles. By conducting Taber experiments, we obtained the estimated abrasive wear coefficients representative of varying seabed topographies and integrated the effects from abrasion and corrosion into cable lifetime prediction. To the best of the authors' knowledge, this was the first study providing power utility and cable industries with the ability to assess cables' lifetime by taking into account scouring, corrosion, and abrasion for different cable constructions and environmental conditions.

Our future research work will focus on exploring robot deployment of low frequency wide band sonar, to capture in-situ interactions between the subsea power cables and the environment, cable displacement, as well as the cables structural integrity. A new multilayer co-centrical scattering theory for subsea cable analysis with low frequency sonar will intend to exploit the returned echo from subsea cable samples at different lifecycle stages, e.g. varying degrees of armour loss and condition of dielectric. Such analysis can then be compared with offline analytical predictions of degradation rates. This type of technology will also provide a new assessment capability into the installation processes of new cables, such as rock dumping on the cable, which may adversely impact cable integrity at the point of installation.

REFERENCES

[1] P. Hokastad, I. B. Utne, and J. Vatn, *Risk and Interdependencies in Critical Infrastructures: A Guideline for Analysis*. London, U.K.: Springer-Verlag, 2012.
[2] P. Bronski *et al.* The economics of load defection. Rocky Mountain Institute. Apr. 2015. Available: https://rmi.org/wp-content/uploads/2017/05/RMI_Document_Repository_Public-Reprts_2015-06_RMI-TheEconomicsOfLoadDefection-ExecSummary.pdf

[3] Department of Energy & Climate Change, "Delivering UK energy investment: Networks," London, U.K., Tech. Rep., Jan. 2015. [Online]. Available: https://assets.publishing.service.gov.uk/government/uploads/system/uploads/attachment_data/le/394509/DECC_Energy

[4] The Crown Estate, "Transmission infrastructure associated with connecting offshore generation," UK Government, London, U.K., Tech. Rep., 2013. [Online]. Available: https://www.transmissioninfrastructure-offshoregen.co.uk/media/9384/the_crown_estate_transmission_infrastructure_print_april.pdf

[5] 4C Offshore. *Western Isles Link Interconnector*. Accessed: Mar. 18, 2019. [Online]. Available: https://www.4coffshore.com/transmission/interconnector-western-islesAQ:link-icid1.htm

[6] 4C Offshore. *NorthConnect*. Accessed: Mar. 18, 2019. [Online]. Available: https://www.4coffshore.com/transmission/interconnector-northconnect-icid12.html

[7] SP Energy Networks. *Western HVDC Link*. Accessed: Oct. 10, 2018. [Online]. Available: https://www.spenergynetworks.co.uk/pages/western_hvdc_link.aspx

[8] Westwood Global Energy Group. (2017). *Offshore Wind Driving 2017-2021 Subsea Cable Market Growth*. [Online]. Available: https://www.offshorewind.biz/2017/02/24/offshore-wind-driving-2017-2021-subsea-cable-demand/

[9] GCube Insurance Services. *An Insurance Buyer's Guide to Subsea Cabling Incidents*. Accessed: Nov. 22, 2018. [Online]. Available: www.gcube-insurance.com/

[10] *On-Bottom Stability Design of Submarine Pipelines*, document DNVGL-RP-F109, May 2017. [Online]. Available: http://rules.dnvgl.com/docs/pdf/dnvgl/RP/2017-05/DNVGL-RP-F109.pdf

[11] The Crown Estate, "PFOW enabling actions project: Sub-sea cable lifecycle study," European Mar. Energy Centre, Orkney, U.K., Tech. Rep., Feb. 2015. [Online]. Available: http://www.thecrownestate.co.uk/media/451414/ei-pfow-enabling-actions-project-subsea-cable-lifecycle-study.pdf.

[12] J. Beale, "Transmission cable protection and stabilisation for the wave and tidal energy industries," in *Proc. 9th Eur. Wave Tidal Energy Conf. (EWTEC)*, Southampton, U.K., Sep. 2011.

[13] T. Worzyk, *Submarine Power Cables: Design, Installation, Repair, Environmental Aspects*. Berlin, Germany: Springer-Verlag, 2009, p. 296. doi: 10.1007/978-3-642-01270-9.

[14] T. A. Holte *et al.*, "Recommendations for mechanical tests on submarine cables," *Electra*, no. 171, pp. 58–68, 1997. [Online]. Available: https://www.cigre.org/

[15] *Tests on Cable Oversheaths Which Have a Special Protective Function and are Applied by Extrusion*, document IEC 60229, 2007. [Online]. Available: https://webstore.iec.ch/publication/1066

[16] F. David, C. Bailey, P. Rajaguru, W. Tang, and C. Yin, "Prognostics and health management of subsea cables," in *Prognostics and Health Management. Prognostics and Health Management of Electronics: Fundamentals, Machine Learning, and the Internet of Things*, M. Pecht and M. Kang, Eds. Hoboken, NJ, USA: Wiley, 2018, ch. 16, pp. 451–478.

[17] J. Larsen-Basse, K. Htun, and A. Tadjvar, "Abrasion-corrosion studies for the Hawaii deep water cable program Phase II-C," Georgia Inst. Technol., Atlanta, GA, USA, Tech. Rep., 1987.

[18] P. S. Wu, "Undersea light guide cable reliability analyses," in *Proc. Rel. Maintainability Symp.*, Los Angeles, CA, USA, Jan. 1990, pp. 157–159.

[19] K. G. Booth, "Abrasion resistance evaluation method for high-density polyethylene jackets used on small diameter submarine cables," Appl. Phys. Lab., Univ. Washington, Seattle, WA, USA, Tech. Rep. APL-UW TR 9303, 1993.

[20] Cablel Hellenic Cables Group. *Submarine Cables Brochure*. Accessed: Mar. 18, 2019. [Online]. Available: http://www.cablel.com/Files/Documents/Document193.File1.Original.pdf

[21] C. Xihao, H. Junhua, and X. Jun, "Position stability of surface laid submarine optical fiber cables," in *Proc. 57th Int. Wire Cable Symp.*, Providence, RI, USA, Nov. 2008, pp. 436–439.

[22] M. I. Friswell, "Steady-state analysis of underwater cables," *J. Waterway, Port, Coastal, Ocean Eng.*, vol. 121, no. 2, pp. 98–104, 1995.

[23] W. P. Graebel, *Engineering Fluid Mechanics*. Boca Raton, FL, USA: CRC Press, 2001, p. 752.

[24] J. Chesnoy, *Undersea Fiber Communication Systems*. San Diego, CA, USA: Academic, 2002.

[25] J. M. Gere and B. J. Goodno, *Mechanics of Materials*, 7th ed. Boston, MA, USA: Cengage Learning, 2008.

[26] A. Burden, R. Burden, and J. Faires, *Numerical Analysis*. Pacific Grove, CA, USA: Brooks/Cole, 2005.

[27] B. M. Sumer and J. Fredsøe, *The Mechanics of Scour in the Marine Environment*. Singapore: World Scientific, 2002, p. 552.

[28] A. K. Arya and B. Shingan, "Scour-mechanism, detection and mitigation for subsea pipeline integrity," *Int. J. Eng. Res. Technol.*, vol. 1, no. 3, pp. 1–14, 2012.

[29] L. Cheng, K. Yeow, Z. Zang, and F. Li, "3D scour below pipelines under waves and combined waves and currents," *Coastal Eng.*, vol. 83, pp. 137–149, Jan. 2014.

[30] L. Cheng, K. Yeow, Z. Zhang, and B. Teng, "Three-dimensional scour below offshore pipelines in steady currents," *Coastal Eng.*, vol. 56, nos. 5–6, pp. 577–590, 2009.

[31] K. G. Budinski, "Resistance to particle abrasion of selected plastics," *Wear*, vols. 203–204, pp. 302–309, Mar. 1997.

[32] G. E. Dieter and L. C. Schmidt, *Engineering Design*, 4th ed. New York, NY, USA: McGraw-Hill, 2009.

[33] S. Qin and W. Cui, "Effect of corrosion models on the time-dependent reliability of steel plated elements," *Mar. Struct.*, vol. 16, no. 1, pp. 15–34, 2003.

[34] *API RP-2SK: Design and Analysis of Station-Keeping Systems for Floating Structures*, 3rd ed., Amer. Petroleum Inst., Washington, DC, USA, 2005.

[35] E. Fontaine, A. Potts, K. T. Ma, A. L. Arredondo, and R. E. Melchers, *SCORCH JIP: Examination and Testing of Severely-Corroded Mooring Chains From West Africa*, in *Proc. Offshore Technol. Conf.*, Houston, TX, USA, Apr./May 2012.

[36] *Materials Selection, Review 3*, document NORSOK M-001, Nov. 2004.

[37] R. Francis, G. Byrne, and H. S. Campbell, "The corrosion of some stainless steels in a marine mud," in *Proc. Int. Nat. Assoc. Corrosion Eng. (NACE)*, San Antonio, TX, USA, Apr. 1999, pp. 1–16.

[38] *Standard Test Method for Abrasion Resistance of Organic Coatings by the Taber Abraser*, Standard ASTM Int. D4060-10, West Conshohocken, PA, USA, 2010. [Online]. Available: https://www.astm.org/DATABASE.CART/HISTORICAL/D4060-10.htm

[39] K. G. Booth, "Abrasion resistance evaluation method for high-density polyethylene jackets used on small diameter submarine cables," Univ. Washington, Seattle, WA, USA, Tech. Rep. APL-UW TR 9303, 1993.

[40] C. Maier and C. Theresa, *Polypropylene: The Definitive User's Guide and Databook*. Norwich, NY, USA: Plastics Design Library, 1998.

[41] P. N. Trinh, "Measurement of Bitumen relaxation modulus with instrumented indentation," M.S. thesis, School Archit. Built Environ., Roy. Inst. Technol., Stockholm, Sweden, 2012.

[42] G. Y. Lee, C. K. H. Dharan, and R. O. Ritchie, "A physically-based abrasive wear model for composite materials," *Wear*, vol. 252, pp. 322–331, Feb. 2002.

[43] Accessed: Mar. 18, 2019. [Online]. Available: https://www.nexans.co.uk/eservice/UK-en_GB/navigate_325963/Submarine_High_Voltage_Cables.html

[44] F. S. Wong, "First-order, second-moment methods," *Comput. Struct.*, vol. 20, no. 4, pp. 779–791, 1985.

[45] W. Tang, H. Pellae, D. Flynn, and K. Brown, "Integrity analysis inspection and lifecycle prediction of subsea power cables," in *Proc. Prognostics Syst. Health Manage. Conf.*, Chongqing, China, Oct. 2018, pp. 105–114.

Authors' photographs and biographies not available at the time of publication.